MATEC Web of Conferences **21**, 04013 (2015)
DOI: 10.1051/matecconf/20152104013

Numerical simulation and experimental investigation of ductile fracture in SPIF using modified GTN model

Shakir Gatea[1], Bin Lu[2,3], Hengan Ou[1,a], and Graham McCartney[1]

[1] Department of Mechanical, Materials and Manufacturing Engineering, Faculty of Engineering, University of Nottingham, Nottingham NG7 2RD, UK
[2] Institute of Forming Technology and Equipment, Shanghai JiaoTong University, Shanghai 200030, China
[3] Department of Mechanical Engineering, University of Sheffield, Sheffield S1 3JD, UK

Abstract. Incremental sheet forming (ISF) is a relatively new flexible forming process with excellent adaptability to CNC milling machines due to the fact that it does not require any high capacity presses or dies of a specific shape and this makes the process cost-effective and easy to automate for various applications. The purpose of this work is to develop a modified Gurson–Tvergaard-Needleman (GTN) model that can be used to predict ductile fracture in the ISF process. The GTN damage constitutive model was implemented in Abaqus/Explicit via a VUMAT user subroutine. Tensile tests and a scanning electron microscope (SEM) were utilized to determine the parameters for the GTN model experimentally. The deformation on the surface of the tensile specimen was measured and observed by using a digital image correlation (DIC) system to evaluate necking and instability in the tensile specimens. Based on the results obtained by the SEM in the affected zone of tensile specimens, a modified GTN model was employed to predict the fracture of a pure titanium hyperbolic cone using the ISF process. A comparative study was carried out by using experimental testing and numerical simulation results of the ISF process to validate the modified GTN model.

1. Introduction

A characteristic feature of single point incremental forming (SPIF) is that a workpiece is formed by the action of a CNC milling machine tool that has a single-point contact with the sheet metal (blank). The blank is fixed by a blank holder that remains at the same height [1]. In this process, a small sized hemispheric tool moves along user-specified tool paths and incrementally creates the desired shape. Many papers have been published in this field which share one goal for improved understanding of material deformation and fracture mechanism of SPIF so as to achieve an ISF part without defects. A theoretical model for different modes of deformation was proposed, which was built upon membrane analysis and ductile damage mechanics [2, 3]. Experimental observations show that the fracture is not

[a] Corresponding author: h.ou@nottingham.ac.uk

preceded by localized necking and the crack develops under tensile meridional stresses acting under stretching conditions and not by plane shearing stresses. An experimental work using a surface 3D digital image correlation showed that the fracture occurred in the uniaxial stretching domain [4]. To predict the occurrence of failure in the AA5052 sheet, Malhotra et al. [5, 6] used explicit FEA with a damage-based fracture model, in which the failure envelope depends on the hydrostatic pressure and the lode angle. It was noticed that the damage evolution was controlled by local bending around the tool and through-thickness shear. An experimental and numerical study was undertaken by Xu et al. [7] to investigate the effect of through-thickness shear on AA5052-H32 sheet formability in SPIF. As a result, the fracture depth of the cone produced by SPIF was bigger than that of the same cone formed by deep drawing. Therefore, the through-thickness shear in deep drawing can be neglected as it is not significant as compared to that obtained from SPIF. W.B Lievers et al. [8] presented a method to determine the void nucleation rate in the ISF process based on density changes using the GTN model. Three automotive aluminium sheet alloys, i.e. AA5754, AA5182 and AA6111, were used to calibrate the void nucleation behaviour. This technique provides a large homogenous deformation area and avoids the large strain and stress gradient associated with smooth or notched tensile specimens. A simplified version of the NUMISHEET 2014 ISF was analysed by Jacob smith et al. [9] using LS-Dyna explicit FEA to implement a shear-modified GTN model, as proposed by Nahshon and Hutchinson. The results show that the shear modification model can have a significant influence on the fracture depth in the ISF process.

In the present study, a VUMAT user subroutine is developed to implement a shear-modified GTN model by Abaqus/explicit; then this model was validated with experimental results. In addition, tensile test with DIC and an SEM were used to determine the modified GTN model parameters.

2. Constitutive model (GTN model)

The classical plasticity theory (the Von-Mises theory) was extended by Gurson [10] to cover the effect of plastic dilatancy and pressure sensitivities of inelastic flow based on the observation that the nucleation and growth of voids in a ductile metal can be described macroscopically. The Tvergaard-Needleman modification (GTN model) [11] is considered one of the most popular versions of Gurson's model. This model introduces a void volume fraction f^* and three constitutive coefficients q_1, q_2 and q_3 characterizing the integration effects between the voids. The yield function of the GTN model takes the following form:

$$\emptyset = \left(\frac{\sigma_q}{\sigma_y}\right)^2 + 2q_1 f^* \cosh\left(-\frac{3q_2 p}{2\sigma_y}\right) - \left(1 + q_3 f^{*2}\right) = 0. \tag{1}$$

Where $\emptyset$ is the non-dilatational strain energy; q_1, q_2 and q_3 are the constitutive parameters proposed by Tvergaard [12] to get closer agreement between the GTN model and the full numerical analyses of a periodic array of voids, and the values of q_1 =1.5, q_2 =1.0 and q_3 =2.25; $\sigma_q = \sqrt{\frac{3}{2} S_{ij} S_{ij}}$ is equivalent to von-Mises stress; $S_{ij} = \sigma_{ij} - \frac{1}{3}\sigma_{ii}$ is a deviatoric stress tensor; $p = -\frac{1}{3}\sigma_{ii}$ is the hydrostatic stress; and σ_y is the flow stress of the undamaged material matrix. The parameter f^* was introduced by Tvergaard-Needleman to account for the final material failure for void coalescence. This parameter is a function of the void volume fraction f and is specified as

$$f^* = \begin{cases} f & if\ f \le f_c \\ f_c + \dfrac{\bar{f}_F - f_c}{f_{f-f_c}}(f - f_c) & if\ f_c < f > f_F \\ \bar{f}_F & if\ f \ge f_F \end{cases} \tag{2}$$

Where f_c denotes the critical value of the void volume fraction, and f_F is the final value of the void volume fraction when the material has completely lost its stress carrying capacity. The function of $\bar{f}_F$ is defined as

$$\bar{f}_F = \frac{q_1 + \sqrt{q_1^2 - q_3}}{q_3}. \tag{3}$$

The increase in the initial void volume fraction f is defined as the sum of the increments due to void nucleation and void growth

$$df = df_{nucleation} + df_{growth}. \tag{4}$$

The nucleation mechanism is considered to be dependent exclusively on the plastic strain of the matrix material and it is assumed that the voids are nucleated only in tension.

$$df_{nucleation} = A d\bar{\varepsilon}_m^p \tag{5}$$

$$\text{where} \quad A = \begin{cases} \dfrac{f_N}{S_N\sqrt{2\pi}} e^{-0.5\left(\frac{d\bar{\varepsilon}_m^p - \varepsilon_N}{S_N}\right)^2} & if\ p \geq 0 \\ 0 & if\ p < 0. \end{cases} \tag{6}$$

The parameter A is defined as a function of the matrix of total equivalent plastic strain ε_m^p, f_N is the void volume fraction of the nucleated void; ε_N is the mean value of the normal distribution of the nucleation strain; and S_N is the standard deviation. $d\bar{\varepsilon}_m^p = \frac{\sigma : d\varepsilon^p}{(1-f)\sigma_y}$ is equivalent plastic strain.

$$df_{growth} = (1 - f) d\varepsilon_{ii}^p \tag{7}$$

where $d\varepsilon_{ii}^p$ is the trace of the plastic strain tensor.

3. Shear mechanism

The GTN model is limited due to the fact that it ignores the fracture mechanism based on shear; many papers have been published recently to develop the GTN model by adding a function to capture the fracture at low stress triaxialities. Xue [13] proposed a function based on the void volume fraction, equivalent plastic strain ε_{eq} and the lode angle θ_L. This mechanism was based on a cell structure subjected to a simple shear strain with a circular void at the centre. Xue's shear mechanism assumes that the increment in the void volume fraction obtained shear effect is

$$df_{shear} = q_4 f^{q_5} g_0 \varepsilon_{eq} \dot{\varepsilon}_{eq}. \tag{8}$$

For a 2D model q_4 =1.69 and q_5 =0.5 or q_4 =1.86 and q_5 =1/3 for 3D problems respectively; ε_{eq} is the total equivalent strain and g_0 is a parameter responsible for the inclusion of the Lode angle dependence on the shear mechanism, which can be defined as:

$$g_0 = 1 - \frac{6|\theta_L|}{\pi} \tag{9}$$

$$\theta_L = \tan^{-1}\left[\frac{1}{\sqrt{3}}\left[2\left(\frac{S_2 - S_3}{S_1 - S_3}\right)\right]\right] \tag{10}$$

where S_1, S_2 and S_3 are the deviatoric stress tensors in the principal plane.

The total void volume fraction after the addition contribution of shear mechanism becomes

$$f_{total} = f_{initial} + (df_{nucleation} + df_{growth} + df_{shear}) \tag{11}$$

Table 1. Mechanical properties of pure titanium.

Yield stress	Ultimate tensile stress	Young's modulus	Poisson's ratio	Density
366 MPa	575 MPa	111.7 GPa	0.34	4505 kg/m^3

4. FEM and algorithm of VUMAT

The modified GTN model has been implemented in Abaqus/explicit through the material user subroutine VUMAT. This analysis employs the GTN model to determine whether plastic deformation occurs. The VUMAT begins by assuming the increment in the strain is purely elastic, and based on this assumption a trial stress is calculated before the yield function is checked. Thus if $\emptyset \leq 0$?, the current state is elastic, so it is necessary to update the stresses and exit; if not, the current state is plastic and the incremental plastic strain should be determined. In this work, the change in plastic strain follows [14, 15]. Figure 1 shows the flow chart of the GTN model stress integration algorithm.

5. Experimental work

5.1 Tensile test

In order to simulate the SPIF process by means of the FEM program, the mechanical properties of sheet metal should be determined. In this work, an INSTRON testing machine was utilized and the specimen design is in accordance with British standard (BS EN 10002-1). Tensile specimens were obtained using an EDM cutting process from pure titanium sheet at 0°, 45° and 90° with respect to the rolling direction. The material characteristics of pure titanium are reported in Table 1. To measure the displacement on the surface of the specimens during tensile tests, a Dantec Q-400 DIC (digital image correlation) system was used.

6. Results and discussion

To evaluate the heterogeneity of deformation and measure the displacement on the surface of the tensile specimens, several tensile tests were conducted with the use of DIC. Figure (2) shows the load displacement curve produced from the tensile test, and the locations for determining the modifications to the GTN model parameters.

6.1 Determination of material parameters of the GTN model

To apply the GTN model in the analysis, it is necessary to determine several microstructure parameters. A scanning electron microscope (SEM) was used to obtain the images of the microstructure and these images were analysed by using *ImageJ* software to determine the void volume fraction at different stages throughout the tensile test. The first step of material examination was to determine the primary void volume fraction by scanning the sheet before plastic deformation. The initial void volume fraction comes from non-metallic inclusions and second-phase particles, as shown in Fig. 3A. These inclusions were randomly distributed in the metal matrix. The initial void volume fraction f is determined as a mean value of non-metallic inclusions and its value is (0.00138).

When the tensile specimen is subjected to plastic strain under the effect of external loading, the nucleation mechanism is started by void formation around the non-metallic inclusions and second-phase particles. Figure 3B shows the volume fraction of nucleated void ($f_N = 0.017$); at this value of f_N the strain of inclusion is $\varepsilon_N = 0.3$ and the standard deviation of the nucleation strain is $S_N = 0.1$. When the load increases and reaches the maximum value (3.04 KN), and displacement reaches (11 mm), significant changes in the dimensions of the tensile specimen can be noticed. Furthermore, the material

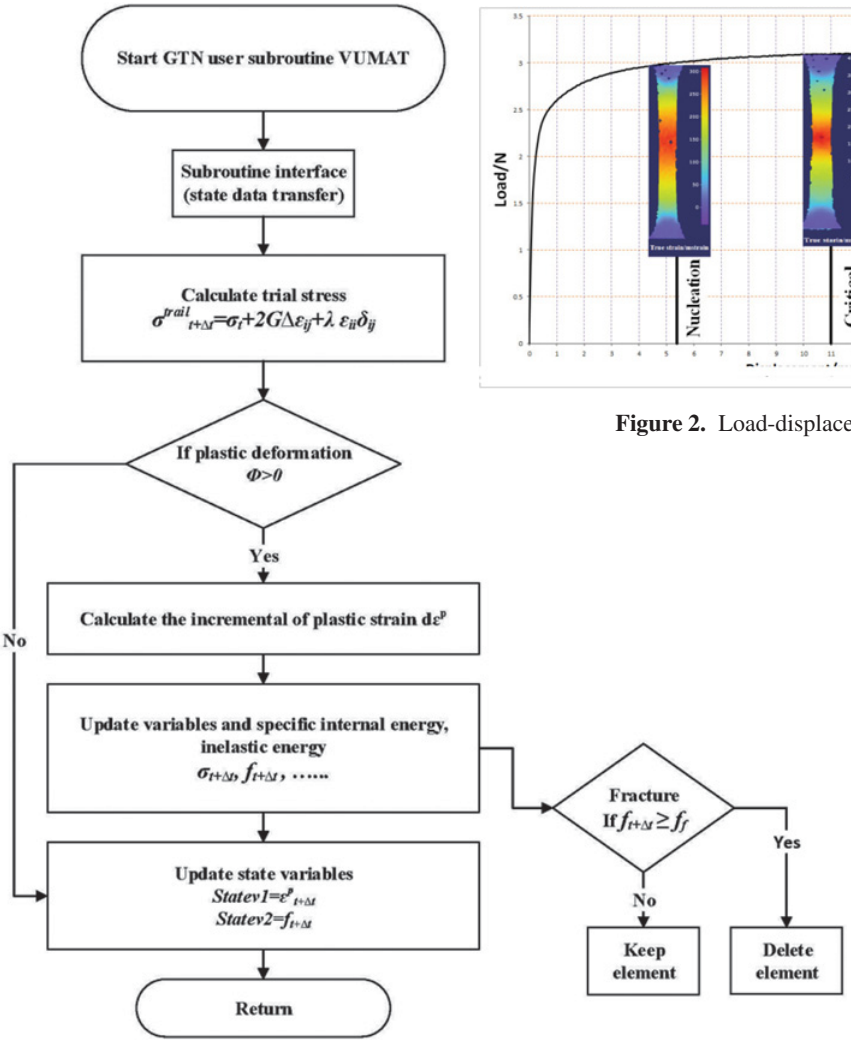

Figure 1. Flowchart of GTN VUMAT.

Figure 2. Load-displacement curve of in tensile test.

bearing capacity is quickly lost and the void volume fraction reaches the critical value f_c (0.2593) (Fig. 3C). When the displacement reaches (18.8 mm), the voids get bigger and tearing of the ligaments between enlarged voids causes fracture in the tensile specimen perpendicular to the tensile loading. The void volume fraction at fracture f_F is evaluated as 0.3025, as shown in Fig. 3D.

6.2 SPIF

A hyperbolic cone is selected to test the GTN model for predicting fracture in SPIF; this part is designed with varying wall angles from 30° to 80° as shown in Fig. 4. The explicit finite element code Abaqus with VUMAT was employed to simulate SPIF and a pure titanium sheet with dimensions 140 × 140 × 0.5 mm is used as an elasto-plastic model and is meshed with an 8 node brick element

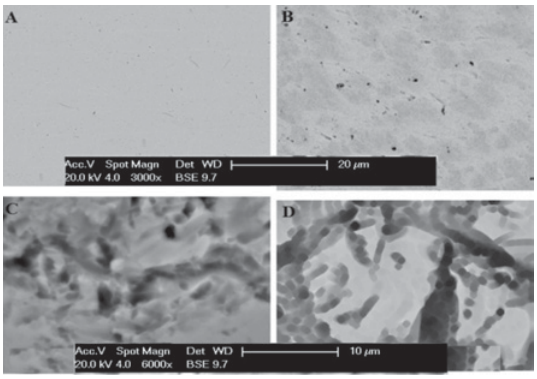

Figure 3. Microstructure of pure titanium at different stages throughout the tensile test.

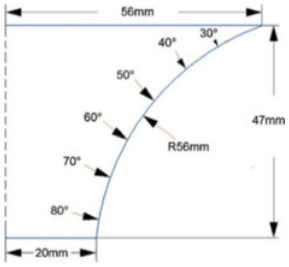

Figure 4. Geometric shape of hyperbolic cone.

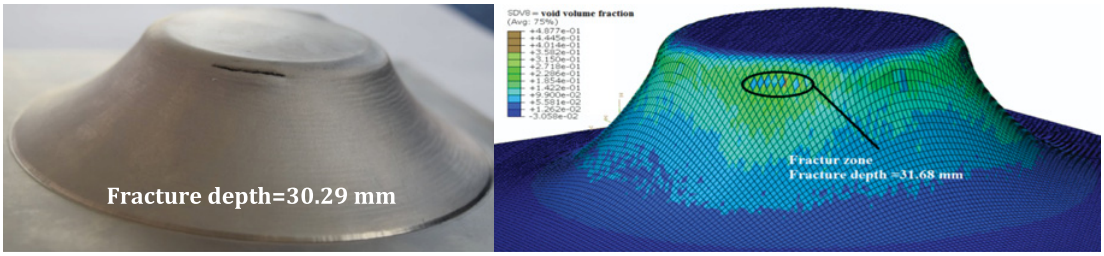

Figure 5. Simulated results in comparison with actual experiments.

(C3D8 full integration). The Ludwik hardening law was used to describe the plastic behaviour of sheet material and given by: $\sigma_y = 366 + 373\varepsilon_{eq}^{0.36}$. The FE results showed that the fracture occurs on the outer side of the wall at the transition area between contact and non-contact zone when the void volume fracture reaches to 0.3025. To check the validation of the VUMAT of the modified GTN-model the FE results were compared with experimental work as shown in Fig. 5. The SPIF simulated results by Abaqus are consistent with experiments, with an error of 4.58%, which demonstrates the capability of the modified GTN model to predict the fracture in SPIF.

7. Conclusions

This work presents an experimental and numerical investigation of ductile fracture in the SPIF. A numerical approach was developed by implementing the modified GTN model in Abaqus/Explicit via a VUMAT user subroutine. A SEM with *imageJ* software was used to determine the modified GTN parameters at different stages throughout the tensile test. The SPIF model with modified GTN-VUMAT showed a good agreement of fracture depth when the numerical results were compared with the experimental work.

This work was supported by the Engineering and Physical Science Research Council of UK (EP/L02084X/1), the Marie Curie International Incoming Fellowship (628,055&913,055), International Research Staff Exchange Scheme (IRSES, MatProFuture project, 318,968) within the 7th EC Framework Programme (FP7).

References

[1] G. Hirt, and M. Bambach, *Incremental Sheet Forming, in Sheet Metal Forming: Processes and Applications*, T. Altan and A.E. Tekkaya, Editors (ASM International, Ohio 2012)
[2] P.A.F. Martins, N. Bay, M. Skjoedt, and M.B. Silva, CIRP Ann. Manuf. Technol., **57**, 247 (2008)
[3] M.B. Silva, M. Skjoedt, P.A.F. Martins, and N. Bay, Int. J. Mach. Tool Manu., **48**, 73 (2008)
[4] Decultot, N., L. Robert, V. Velay, and G. Bernhart, EPJ Web of Conferences, **6**, 11001 (2010)
[5] R. Malhotra, L. Xue, J. Cao, and T. Belytschko, NUMISHEET, **1383**, 469 (2011)
[6] R.Malhotra, L. Xue, T. Belytschko, and J. Cao, J. Mater. Process. Technol., **212**, 1573 (2012)
[7] D. Xu, R. Malhotra, J. Chen, B. Lu, and J. Cao, NUMIFORM, **1532**, 969 (2013)
[8] W.B. Lievers, A.K. Pilkey, and D.J. Lloyd, Acta Mater., **52**, 3001 (2004)
[9] J. Smith, R. Malhotra, W.K. Liu, and J. Cao, NUMISHEET, **1567**, 824 (2013)
[10] A.L. Gurson, J. Eng. Mater. Technol., **99**, 2 (1977)
[11] V. Tvergaard, and A. Needleman, Acta Metall., **32**, 157 (1984)
[12] V. Tvergaard, , J. Mech. Phys. Solids, **30**, 399 (1982)
[13] L. Xue, Eng. Fract. Mech., **75**, 3343 (2008)
[14] M. Ortiz, and J. Simo, Int. J. Nume. Meth. Eng., **23**, 353 (1986)
[15] B.E. Engelmann, and R.G. Whirley, Nucl. Eng. Des., **138**, 138 (1992)